Chapter 2
Fundamentals

This chapter briefly reviews the basics that are required for the theoretical investigations and the practical implementations in this monograph. That comprises fundamentals in kinematics and dynamics (Sect. 2.1), active control for compliant interaction behavior (Sect. 2.2), and details on the hardware and modeling assumption on the wheeled humanoid robot Rollin' Justin, which has been chosen as the platform for the experimental validations (Sect. 2.3).

2.1 Robot Kinematics and Dynamics

The following sections introduce some basic kinematic and dynamic matters of special importance in the context of this work. For a complete and more detailed version the reader is referred to the standard literature [Pau83, Cra89, Yos90, MLS94, KD02, SK08].

Most robotic designs are based on revolute joints rather than prismatic joints. Thus, one has to deal with torques instead of forces on joint level. In this book the term *joint torque* is mostly used, but the extension to generalized joint forces (including forces and torques) can be made. By default, external loads are referred to as *external forces* since physical contact usually occurs from contact surface to contact surface, hence a force is more common. However, the extension to generalized external forces (including forces and torques) can be made without loss of generality. The simplified notations are used for the sake of brevity.

2.1.1 Forward Kinematics, Jacobian Matrices, and Power Ports

A typical robotic system is described by $\boldsymbol{q} \in \mathbb{R}^n$ joint coordinates, where n is the number of degrees of freedom (DOF). The operational space, e.g. the

A. Dietrich, *Whole-Body Impedance Control of Wheeled Humanoid Robots*,
Springer Tracts in Advanced Robotics 116, DOI 10.1007/978-3-319-40557-5_2

workspace of the end-effector, is usually described by $m \leq n$ coordinates denoted $\boldsymbol{x}(\boldsymbol{q}, \mathcal{L}) \in \mathbb{R}^m$. The kinematic parameterization $\mathcal{L}$ is usually constant and disregarded in the notations. The robot is assumed to be rigid, the only relative motion is along/about the n joint axes.

The most common representation of $\boldsymbol{x}(\boldsymbol{q})$ is in Cartesian coordinates. If $m = n$, then the robot is called non-redundant w. r. t. the operational space with dimension m. If $m < n$, then the manipulator is kinematically redundant and can execute additional tasks by utilizing the $(n-m)$-dimensional *null space* while not disturbing the operational space task.[1] The forward kinematics of the considered robot are described by the mapping $\boldsymbol{q} \mapsto \boldsymbol{x}$, while the inverse kinematics $\boldsymbol{x} \mapsto \boldsymbol{q}$ in a redundant robot is ambiguous and requires additional constraints to be resolved.

The differential and velocity relation between the joint space and the operational space

$$\Delta \boldsymbol{x}(\boldsymbol{q}) = \frac{\partial \boldsymbol{x}(\boldsymbol{q})}{\partial \boldsymbol{q}} \Delta \boldsymbol{q} = \boldsymbol{J}(\boldsymbol{q}) \Delta \boldsymbol{q}, \tag{2.1}$$

$$\dot{\boldsymbol{x}}(\boldsymbol{q}, \dot{\boldsymbol{q}}) = \boldsymbol{J}(\boldsymbol{q}) \dot{\boldsymbol{q}}, \tag{2.2}$$

necessitates a further quantity $\boldsymbol{J}(\boldsymbol{q}) \in \mathbb{R}^{m \times n}$, the Jacobian matrix. The total time derivative $d\{\}/dt$ of a function $\{\}$ is abbreviated as $\dot{\{\}}$ in this book. Based on the geometric point of view (2.1) and (2.2), one can find a simple relation between operational space forces $\boldsymbol{F} \in \mathbb{R}^m$ and joint torques $\boldsymbol{\tau} \in \mathbb{R}^n$:[2]

$$\boldsymbol{\tau} = \boldsymbol{J}(\boldsymbol{q})^T \boldsymbol{F} \tag{2.3}$$

The application of joint torques with (2.3) is called a *Jacobian transposed* approach. This concept is adopted here and constitutes a basic prerequisite for the methods developed in the later chapters. The variables in (2.2) and (2.3) describe either a flow ($\dot{\boldsymbol{q}}$ or $\dot{\boldsymbol{x}}$) or an effort ($\boldsymbol{\tau}$ or $\boldsymbol{F}$). The associated terms build *power ports*, since they define a power through $\dot{\boldsymbol{q}}^T \boldsymbol{\tau}$ and $\dot{\boldsymbol{x}}^T \boldsymbol{F}$, respectively. Via such a port, the system can exchange energy with its environment. All relations are illustrated in Fig. 2.1.

2.1.2 Derivation of the Equations of Motion

Two basic formalisms are briefly reviewed that yield the dynamic equations of a robot. These sections explain the derivation in a nutshell only. A more detailed version can be found in the standard literature listed in Sect. 2.1.

---

[1] Motions in the null space are also denoted *internal motions*.

[2] Note that $\boldsymbol{F}$ may also contain torques, e.g. in the case of a full operational space wrench $\boldsymbol{F} \in \mathbb{R}^6$ with three forces and three torques. Furthermore, $\boldsymbol{\tau}$ may also contain force elements in case of prismatic joints.

Fig. 2.1 Relations between $\dot{\boldsymbol{x}}$, $\boldsymbol{F}$, $\dot{\boldsymbol{q}}$, and $\boldsymbol{\tau}$ for a redundant manipulator with $m < n$

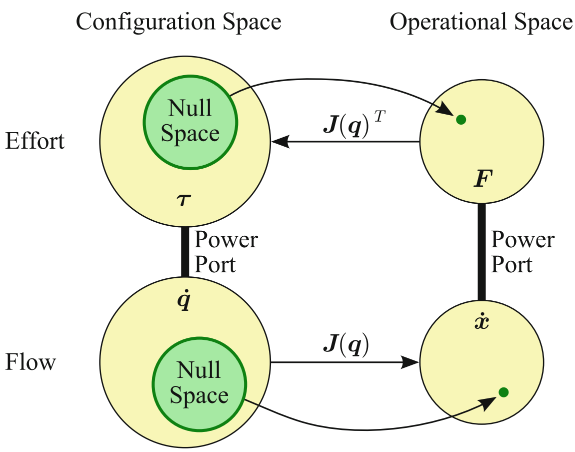

2.1.2.1 Lagrange Formalism

The Lagrange formalism is an energy-based technique to obtain the dynamic equations. An n-DOF system with joint values $\boldsymbol{q} \in \mathbb{R}^n$ and joint velocities $\dot{\boldsymbol{q}} \in \mathbb{R}^n$ is described by the so-called Lagrangian

$$L(\boldsymbol{q}, \dot{\boldsymbol{q}}) = T(\boldsymbol{q}, \dot{\boldsymbol{q}}) - V(\boldsymbol{q}), \tag{2.4}$$

which is given by the kinetic energy $T(\boldsymbol{q}, \dot{\boldsymbol{q}})$ of the system minus its potential energy $V(\boldsymbol{q})$. Then the dynamic equations can be obtained by evaluating

$$\frac{d}{dt}\left(\frac{\partial L(\boldsymbol{q}, \dot{\boldsymbol{q}})}{\partial \dot{\boldsymbol{q}}}\right)^T - \left(\frac{\partial L}{\partial \boldsymbol{q}}\right)^T = \boldsymbol{Q}. \tag{2.5}$$

The vector $\boldsymbol{Q} \in \mathbb{R}^n$ contains the generalized joint forces $\boldsymbol{\tau} \in \mathbb{R}^n$, the external loads $\boldsymbol{\tau}_{\text{ext}} \in \mathbb{R}^n$, and non-conservative generalized forces such as friction. The main advantage of the method is the simple analytical determination of the kinetic and potential energy. But the computational burden of the method makes it unsuitable for large systems with many DOF. The computational effort for an n-link robot is of order $\mathcal{O}(n^4)$ while it is only $\mathcal{O}(n)$ with the iterative Newton–Euler formalism. See [Yos90] for a more detailed comparison.

2.1.2.2 Iterative Newton–Euler Formalism

The iterative Newton–Euler algorithm requires the evaluation of Euler's first and second law for each link of the robot. All constraining forces have to be calculated explicitly. Finally, the equations of all links are combined and the constraining forces are eliminated again. The exact procedure will not be detailed here. Fore more information refer to the literature listed in the beginning of Sect. 2.1.

2.1.3 *Rigid Body Dynamics*

The dynamic equations of a rigid robot with n DOF can be written as

$$\boldsymbol{M}(\boldsymbol{q})\ddot{\boldsymbol{q}} + \boldsymbol{C}(\boldsymbol{q}, \dot{\boldsymbol{q}})\dot{\boldsymbol{q}} + \boldsymbol{g}(\boldsymbol{q}) = \boldsymbol{\tau} + \boldsymbol{\tau}_{\mathrm{ext}}. \tag{2.6}$$

The symmetric and positive definite inertia matrix $\boldsymbol{M}(\boldsymbol{q}) \in \mathbb{R}^{n\times n}$ depends on the joint configuration[3] $\boldsymbol{q} \in \mathbb{R}^n$. Gravity effects are contained in $\boldsymbol{g}(\boldsymbol{q}) = (\partial V_{\mathrm{g}}(\boldsymbol{q})/\partial \boldsymbol{q})^T \in \mathbb{R}^n$, where $V_{\mathrm{g}}(\boldsymbol{q})$ denotes the gravity potential. Coriolis/centrifugal forces and torques are represented by $\boldsymbol{C}(\boldsymbol{q}, \dot{\boldsymbol{q}})\dot{\boldsymbol{q}} \in \mathbb{R}^n$. The generalized forces[4] $\boldsymbol{\tau} \in \mathbb{R}^n$ describe the control inputs. Generalized external forces are denoted by $\boldsymbol{\tau}_{\mathrm{ext}} \in \mathbb{R}^n$. The matrix $\boldsymbol{C}(\boldsymbol{q}, \dot{\boldsymbol{q}})$ is not unique in general, but it can be chosen according to the Christoffel symbols [MLS94] such that it complies with the relation

$$\dot{\boldsymbol{M}}(\boldsymbol{q}, \dot{\boldsymbol{q}}) = \boldsymbol{C}(\boldsymbol{q}, \dot{\boldsymbol{q}}) + \boldsymbol{C}(\boldsymbol{q}, \dot{\boldsymbol{q}})^T \tag{2.7}$$

which is in turn equivalent to the skew symmetry of $\dot{\boldsymbol{M}}(\boldsymbol{q}, \dot{\boldsymbol{q}}) - 2\boldsymbol{C}(\boldsymbol{q}, \dot{\boldsymbol{q}})$. This property is crucial for showing passivity of (2.6) w. r. t. input $(\boldsymbol{\tau} + \boldsymbol{\tau}_{\mathrm{ext}})$ and output $\dot{\boldsymbol{q}}$ and the total energy $\frac{1}{2}\dot{\boldsymbol{q}}^T\boldsymbol{M}(\boldsymbol{q})\dot{\boldsymbol{q}} + V_{\mathrm{g}}(\boldsymbol{q})$ as the storage function. This representation of the Coriolis/centrifugal matrix will be used by default in this book.

2.2 Compliant Motion Control of Robotic Systems

Featuring compliant behavior is an important requirement in many robotic applications. Consider task execution in unknown, dynamic, and unstructured environments such as households, or the cooperation of humans and robots in the same workspace. Whenever a physical contact between the robot and its environment occurs, the interaction behavior should be compliant or at least properly specified in terms of forces and torques. Two fundamental approaches exist to realize compliance: active control and the use of passive elements such as mechanical springs. Only the controlled compliance will be addressed in this book, whereas passive compliance is a matter of construction and mechanical design of the robot.

In the seminal work of Hogan [Hog85], the nature of physical systems is described from the environment point of view. They appear either as *admittances* accepting effort input (force) and yielding flow output (motion) or *impedances* accepting flow

[3]Positions for prismatic joints and angles for revolute joints.

[4]Forces for prismatic joints and torques for revolute joints.

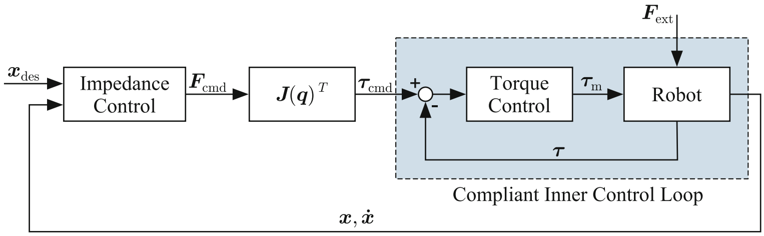

Fig. 2.2 Impedance control in the operational space $x \in \mathbb{R}^m$ with $m < n$

input (motion) and yielding effort output (force). His second fundamental statement is that dynamic interaction between physical systems cannot be controlled by exclusively commanding the position *or* the force. A controller has to incorporate the relation between these port variables as well. In this section the two classical approaches of impedance and admittance control for active compliance are briefly recapitulated. Especially impedance control [ASOH07, OASKH08] is of major importance in this monograph since the theory and the implementation of various impedance-based methods are addressed.

2.2.1 Impedance Control

The goal of impedance control is to alter the mechanical impedance of the robot, that is, the mapping from (generalized) velocities to (generalized) forces [Ott08]. Since the environment can be physically described as an admittance [Hog85] that maps forces to velocities, impressing an impedance behavior on the manipulator is a proper choice to define the interaction behavior in contact.

Figure 2.2 depicts the impedance control regulation case with setpoint $\boldsymbol{x}_{\text{des}}$ (des: desired) in the operational space $\boldsymbol{x} \in \mathbb{R}^m$ with $m < n$, for example in the Cartesian coordinates of the end-effector. This desired value is sometimes also called the virtual equilibrium. It is reached in the case of free motion, i.e. in the absence of external forces. By feeding the robot motion back, one computes the necessary force $\boldsymbol{F}_{\text{cmd}}$ (cmd: command) to implement the prescribed impedance. A kinematic mapping via the transpose of the Jacobian matrix $\boldsymbol{J}(\boldsymbol{q}) = \partial \boldsymbol{x} / \partial \boldsymbol{q}$ yields the required torque $\boldsymbol{\tau}_{\text{cmd}}$. The inner control loop realizes this torque by feedback of $\boldsymbol{\tau}$ under the influence of an external force $\boldsymbol{F}_{\text{ext}} \in \mathbb{R}^m$.[5] The impedance causality is $\dot{\boldsymbol{x}} \to \boldsymbol{F}_{\text{ext}}$, so repositioning the robot in the operational space results in forces acting on the environment.

When considering the overall structure of the impedance control in Fig. 2.2, one can conclude that the inner torque control loop is compliant while the outer loop

[5] In general, an external torque $\boldsymbol{\tau}_{\text{ext}} \in \mathbb{R}^n$ acts on the robot. If the contact with the environment is closed in the operational space, e.g. at the end-effector with coordinates $\boldsymbol{x}$, the force $\boldsymbol{F}_{\text{ext}} \in \mathbb{R}^m$ with $m < n$ is sufficient to describe the external load.

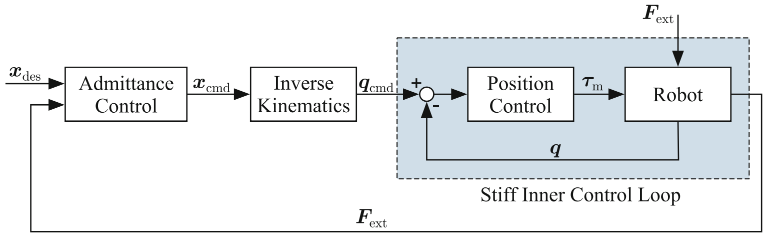

Fig. 2.3 Admittance control in the operational space $\boldsymbol{x} \in \mathbb{R}^m$ with $m < n$

increases the stiffness of the complete system. The torque feedback in the inner loop allows for good contact behavior for small and medium stiffness in the impedance law. However, further increasing the stiffness will ultimately destabilize the system. Another characteristic of the impedance is the absence of an integrator. The controller has basically a PD structure. The inevitable steady-state error $\boldsymbol{x}_{\text{des}} - \boldsymbol{x}$ for $t \to \infty$ in the presence of model uncertainties or external loads can be reduced by increasing the stiffness. While the regulation case is depicted here, the tracking performance in case of a desired trajectory $\boldsymbol{x}_{\text{des}}(t)$ can be improved by adding a feed-forward term taking $\ddot{\boldsymbol{x}}_{\text{des}}(t)$ and the corresponding reflected inertia into account.

Compliance control is a special case of impedance regulation control, where the focus is put on the realization of a desired contact stiffness and damping [Ott08]. Compared to approaches based on the classical OSF [Kha87], where the perceived inertia is actively modified, the natural inertia of the robot is preserved in compliance control. The main advantage of the method is that the feedback of the generalized external forces is not required, which is beneficial in terms of robustness, availability of measurements, and the complexity of the implementation [OKN08].

2.2.2 Admittance Control

A mechanical admittance is the inverse of a mechanical impedance, that is, the mapping from (generalized) forces to (generalized) velocities. In compliant admittance control of robots, one employs a position or velocity controller in combination with explicit measurement and feedback of the generalized external forces. Figure 2.3 illustrates the implementation of such an admittance with joint position control interface. A typical example is Cartesian admittance control, where the external forces $\boldsymbol{F}_{\text{ext}}$ are measured at the tip of the end-effector by a six-axis force-torque sensor. As a result, compliance will only be achieved at the end-effector after this sensor, whereas the structure of the robot will react stiff in case of physical interaction.[6]

[6]One can also implement a compliant admittance controller on joint level via joint torque sensing, which would then lead to compliance along the entire manipulator.

The admittance subsystem yields a position $\boldsymbol{x}_{\text{cmd}}$ or velocity $\dot{\boldsymbol{x}}_{\text{cmd}}$ to be commanded. Then an inverse kinematics algorithm has to be employed to resolve the kinematic redundancy for $m < n$. The computed reference commands $\boldsymbol{q}_{\text{cmd}}$ or $\dot{\boldsymbol{q}}_{\text{cmd}}$, respectively, are realized in the inner position or velocity control loop. Since the admittance causality is $\boldsymbol{F}_{\text{ext}} \rightarrow \dot{\boldsymbol{x}}_{\text{cmd}}$, external forces result in a repositioning of the manipulator.

When considering the overall structure of the admittance control in Fig. 2.3, one can conclude that the inner position control loop is stiff, while the outer loop is responsible for the compliance. The inner-loop controller allows for high positioning accuracy, especially for medium and high stiffness. However, decreasing the stiffness will ultimately destabilize the system, which is a direct result of the admittance causality. Another restriction on its compliant contact behavior is the non-collocated feedback of the external forces in cases such as the Cartesian admittance control discussed above. The admittance-controlled system may involve substantial dynamics between actuator and sensor, which can lead to contact instability [CH89]. Admittance control is frequently used in robots which do not provide joint torque sensing or direct motor current interfaces [Ott08].

2.3 Humanoid Robot Rollin' Justin

The experiments in this book are mainly carried out on the wheeled humanoid robot Rollin' Justin[7] [OEF+06, BOW+07, BWS+09], see Fig. 2.4 (right). In Sect. 2.3.1, its hardware is presented as well as the underlying design principles. Section 2.3.2 summarizes several modeling assumptions that have to be made with regard to the implementation of the methods developed in this book.

2.3.1 Design and Hardware

The concept of Rollin' Justin is based on the principles of modularity and integrated design. In order to pass standard doorways, the overall width of the robot can be reduced to about 0.9 m by adjusting the upper body configuration and retracting the wheels. In terms of workspace, the robot is able to reach the floor as well as objects up to a height of about 2.7 m. The robot has an anthropomorphic structure which facilitates the operation in human environment where furniture, tools, and objects are optimized for the human anatomy. Another key feature of Rollin' Justin is that the robot can be operated without any cables that would restrict the mobility. It is equipped with a battery and all electronic components and computers are located onboard. Via WLAN and sensor feedback (speech recognition, visual information,

[7] The upper body of Justin was finished *just in* time for its first public presentation at the AUTOMATICA trade fair 2006 in Munich [OEF+06].

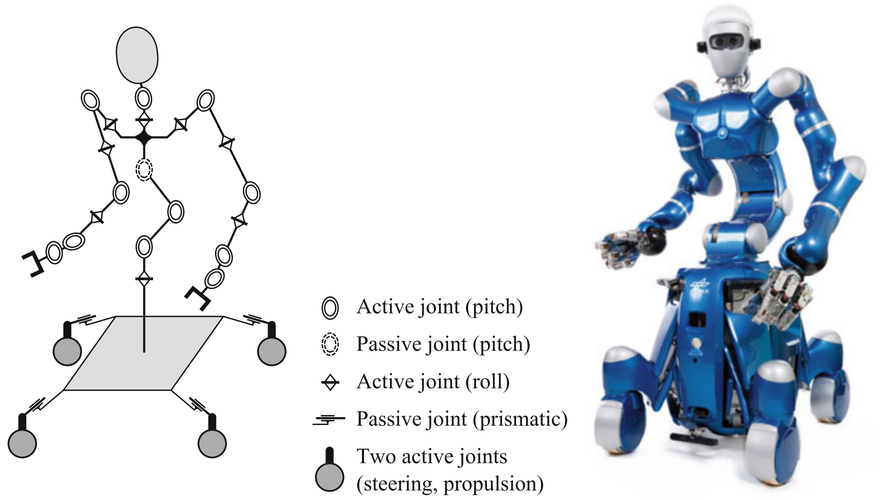

Fig. 2.4 Schematic (*left*) and picture (*right*) of the humanoid robot Rollin' Justin. The hands (12 actuated DOF each) are not specified in the sketch

force feedback), the robot has a permanent interface to the user and the environment during autonomous operation.

The arms are slightly modified versions of the DLR lightweight robots (LWR) of generation III [HSAS+02] with a total weight of 14 kg each. All electronic components are integrated in the arms. As with the human archetype, the arm has seven DOF. They are arranged in a roll-pitch-roll-pitch-roll-pitch-pitch order as it can be seen in the sketch in Fig. 2.4 (left). A payload of 15 kg can be lifted during slow motions and about 7 kg can be handled at maximum velocity. The hands of Rollin' Justin are the DLR Hands II [BGLH01] with four fingers and three actuated DOF per finger. An additional actuator has been integrated in the palm to reconfigure the alignment of the thumb, dependent on the application (power grasp, precision grasp). The head of Rollin' Justin is a pan-tilt unit that is equipped with several sensors, e.g. cameras for stereo vision and scene analysis or an inertial measurement unit for equilibrioception. The torso of Rollin' Justin has three actuated DOF and a kinematically coupled fourth one. The whole upper body weighs about 45 kg. Except for the two neck joints, all actuated upper body joints are equipped with link-side torque sensors as well as position sensors. This full state feedback makes it possible to implement various control techniques. The joint torque controller operates at a sampling rate of 3 kHz and the main control loop[8] runs at 1 kHz.

The mobile base with about 150 kg contains computers, battery, electronics and so forth [BWS+09]. Rollin' Justin has a variable footprint thanks to its extendable legs. A parallel mechanism ensures that the height of the platform remains unchanged.

[8] The main control loop contains all algorithms above the joint level such as Cartesian impedance control, self-collision avoidance, or online inverse kinematics.

Table 2.1 Actuated degrees of freedom and available control interfaces on Rollin' Justin

Subsystem	DOF	Control interface
Torso	3	Torque, position
Arms	2×7	Torque, position
Hands	2×12	Torque, position
Neck	2	Position
Platform and legs	8	Position, velocity
Total sum	51	

The leg extension DOF are not individually actuated, a reconfiguration is subject to steering and motion of the respective wheel. The leg lengths can also be locked mechanically. Due to the nonholonomy a dynamic feedback linearization is applied to move the platform [GFASH09]. This kinematic control method allows to realize arbitrary motions in the two translational directions forward/backward and left/right, and the rotation about the vertical axis. All actuated DOF of Rollin' Justin are summarized in Table 2.1.

2.3.2 Modeling Assumptions

Several assumptions concerning Rollin' Justin have to be made so that the approaches in this book can be applied to the robot.

Assumption 1 *The motors can be considered as ideal torque sources.*

The electrical time constants of the motors are sufficiently smaller than the mechanical ones. Therefore, one can neglect the electrical dynamics and assume ideal torque sources [Wim12, Ott08].

Assumption 2 *The reduced apparent motor inertia of the torque-controlled manipulator appears rigidly connected to the link inertia.*

The assumption is based on a singular perturbation argumentation applied to the flexible-joint model with large joint stiffness [Ott08, WO12, Wim12] and includes the so-called "inertia shaping" (downscaling of the apparent motor inertia via torque feedback) [OASK+04, ASOH04]. A fast time-scale inner torque controller is embedded in rigid body dynamics of slow time-scale. The apparent link inertia is modified by active control and the singular perturbation argumentation allows to neglect the dynamics between motor and link, resulting in a direct torque input available in the link dynamics as in (2.6).

Assumption 3 *The robot structure is rigid. Motions are restricted to the joints.*

The robot has a lightweight structure and is flexible in the links. Nevertheless, this link flexibility is negligible compared to the joint flexibility which originates from the Harmonic Drive gears and the strain-gauge-based torque sensors. Therefore, a flexible-joint model with concentrated elasticity in the joints can be assumed instead of an infinite-dimensional elastic-link robot model [Ott08].

Assumption 4 *The joint stiffness originating from the Harmonic Drive gears and the torque sensors in the joints is sufficiently high, such that the use of the motor positions instead of link positions for the kinematics does not lead to any noteworthy errors. The only exception concerns gravitational effects.*

Although the joint stiffness is high, gravity leads to deflections between motor and link. In order to compensate for gravity forces and torques properly, one has to take that flexibility into account. That can be realized by employing a *static equivalent of the link position* in the gravity model, which only depends on the motor position [OASK+04, ASOH07]. In order to remain in a passivity-based framework with collocated feedback, the motor position is used in the feedback controller. Once gravity is compensated as described, the dynamics between motor and link are neglected so that the motor positions (instead of the link positions) can be used for any link-side-dependent task definition or control task.

Assumption 5 *The rigid body dynamics* (2.6) *approximate the equations of motion of the flexible-joint model of Rollin' Justin, where the motor positions and the motor torques can be used instead of* $\boldsymbol{q}$ *and* $\boldsymbol{\tau}$*, respectively.*

The assumption of a direct torque input on link side is made possible by Assumptions 1 and 2, the assumption of rigid bodies is validated by Assumption 3, and the use of motor positions as a substitute for link positions is covered by Assumption 4.

Springer
http://www.springer.com/978-3-319-40556-8

Whole-Body Impedance Control of Wheeled Humanoid
Robots
Dietrich, A.
2016, XV, 187 p. 82 illus., 71 illus. in color., Hardcover
ISBN: 978-3-319-40556-8